Acta Cryst. (1995). B51, 1063–1068

Correlation of the Crystal Structures of Diastereomeric Artemisinin Derivatives with Their Proton NMR Spectra in $CDCl_3$

BY JEAN M. KARLE* AND AI. J. LIN

Departments of Pharmacology and Medicinal Chemistry, Division of Experimental Therapeutics, Walter Reed Army Institute of Research, Washington, DC 20307-5100, USA

(*Received* 7 *October* 1994; *accepted* 25 *April* 1995)

Abstract

Large differences were observed in the ^1H NMR chemical shift pattern of the protons adjacent to the ether linkages of two diastereomeric artemisinin derivatives. These differences can be explained by the shielding/deshielding effects of the nitrophenyl group on these protons. The crystal structures of these diastereomers (one as the ethyl ester and the other as the acid analog) showed that the nitrophenyl group is positioned on opposite sides of the fused ring system in the two diastereomers. The upfield or downfield ^1H NMR signal of the protons adjacent to the ether linkages [H(10) and H(12)] of the individual diastereomers correlates with whether the phenyl ring sits under or beside the proton. The crystal structure of the acid analog contains an infrequently observed intermolecular hydrogen bond between the carboxylic acid proton and an ether O atom [O(11)]. However, since the NMR spectra in solution are consistent with the crystal structures, packing forces do not appear to be responsible for the orientation of the nitrophenyl group.

Introduction

The diastereomers (I) and (II) (Fig. 1) are synthetic analogs of the antimalarial agent artemisinin (also called qinghaosu), an endoperoxide-containing sesquiterpene lactone isolated from the Chinese herb *Artemisia annua*. The structure of artemisinin (see Fig. 1) contains a lactone carbonyl group instead of the ether group. Artemisinin, although an effective antimalarial agent, is sparingly soluble in either oil or water and thus was administered orally or by intramuscular injection as an oil (Klayman, 1985). The diastereomers (I) and (II) were synthesized in an effort to design analogs with better solubility, longer plasma half life and higher antimalarial activity than artemisinin.

The NMR spectra for the H(10) and H(12) atoms of the diastereomers (I) and (II) exhibit large differences in the chemical shifts. The differences in chemical shifts for H(10) and H(12) are 0.54 and 0.80 p.p.m., respectively. In addition, the signal for H(12) is further downfield than the signal for H(10) in diastereomer (I). In diastereomer (II) the opposite occurs, with the signal for H(10) being further downfield than the signal for H(12). To understand these large differences in the NMR spectra of (I) and (II), the crystal structures of (I) (as the acid) and (II) were determined. Examination of the crystalline conformation of the diastereomers showed that the chemical shift pattern of the proton NMR spectra of the diastereomers can be explained by the relative position of the nitrophenyl ring to the H(10) and H(12) atoms.

Experimental

Preparation and NMR

Diastereomers (I) and (II) and β-arteether were all derived from the natural product artemisinin without affecting the chiral centers of the fused ring system. All NMR spectra were recorded on a Bruker 300 MHz spectrometer using $CDCl_3$ as solvent and tetramethylsilane as the internal standard.

^1H NMR spectrum of ethyl 3(*R*)-(*p*-nitrophenyl)-3-(10β-dihydroartemisininoxy)propionate (I): δ 8.22 [*d*, 2H, $J = 8.7$ Hz, *H*(21) and *H*(23)], 7.55 [*d*, 2H,

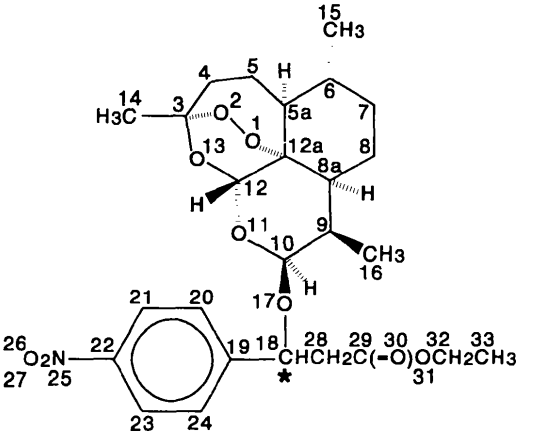

(I) *R* configuration at C(18)
(II) *S* configuration at C(18)

Fig. 1. Chemical structures and numbering scheme of the diastereomers (I) and (II).

* To whom correspondence should be addressed.

$J = 8.7$ Hz, $H(20)$ and $H(24)$], 5.59 [s, 1H, $H(12)$], 5.50 [dd, 1H, $J = 9.8$ and 4.1 Hz, $H(18)$], 4.56 [d, 1H, $J = 3.5$ Hz, $H(10)$], 4.08–4.21 (m, 2H, CH_2CH_3), 2.81 [dd, 1H, $J = 9.8$ and 15 Hz, $H(28)$], 2.63 [dd, 1H, $J = 4.1$ and 15 Hz, $H(28)$], 2.52–2.63 [m, 1H, $H(9)$], 2.3–2.45 (dt, 1H, $J = 4$ and 14 Hz), 1.17–2.1 (m), 1.44 [s, 3H, $H(14)$], 1.28 (t, 3H, $J = 7.1$ Hz, CH_2CH_3), 0.98 [d, 3H, $J = 6.3$ Hz, $H(15)$] and 0.88 [d, 3H, $J = 7.4$ Hz, $H(16)$], 0.87–1.02 (m, 2H).

^{1}H NMR spectrum of ethyl 3(*S*)-(*p*-nitrophenyl)-3-(10β-dihydroartemisininoxy)propionate (II): δ 8.23 [d, 2H, $J = 8.7$ Hz, $H(21)$ and $H(23)$], 7.56 [d, 2H, $J = 8.7$ Hz, $H(20)$ and $H(24)$], 5.22 [dd, 1H, $J = 9$ and 5.5 Hz, $H(18)$], 5.10 [d, 1H, $J = 3.5$ Hz, $H(10)$], 4.79 [s, 1H, $H(12)$], 4.04–4.18 (m, 2H, CH_2CH_3), 2.85 [dd, 1H, $J = 9$ and 15.5 Hz, $H(28)$], 2.61 [dd, 1H, $J = 5.5$ and 15.5 Hz, $H(28)$] 2.6–2.7 [m, 1H, $H(9)$], 2.21–2.34 (dt, 1H, $J = 3.7$ and 14 Hz), 1.08–1.97 (m), 1.32 [s, 3H, $H(14)$], 1.24, (t, 3H, $J = 7$ Hz, CH_2CH_3), 0.94 (d, 3H, $J = 5.4$ Hz, CH_3), 0.91 (d, 3H, $J = 5.8$ Hz, CH_3), 0.81–0.99 (m, 2H).

^{1}H NMR spectrum of β-arteether: δ 5.41 [s, 1H, $H(12)$], 4.80 [d, 1H, $J = 3.5$ Hz, $H(10)$], 3.80–3.93 (m, 1H, CH_2CH_3), 3.40–3.50 (m, 1H, CH_2CH_3), 2.56–2.67 [m, 1H, $H(9)$], 2.37 [dt, 1H, $J = 4$ and 14 Hz, $H(8a)$], 2.03 [dt, 1H, $J = 2.5$ and 14.5 Hz, $H(5a)$], 1.20–1.93 (m), 1.43 [s, 3H, $H(14)$], 1.18 (t, 3H, $J = 7$ Hz, CH_2CH_3), 0.95 [d, 3H, $J = 6.2$ Hz, $H(15)$] and 0.90 [d, 3H, $J = 7.5$ Hz, $H(16)$].

The acid form of diastereomer (I) was obtained by hydrolysis of the corresponding ethyl ester. Crystals of (I) were grown from ethanol/water. Crystals of (II) were grown from hexane.

The structures were solved routinely by direct phase determination (Karle & Karle, 1966). All the non-H atoms were found in the first E map. All the H atoms were placed in idealized positions with a fixed bond length of 0.96 Å, except for H(31) in (I) whose coordinates were derived from the difference map. Anisotropic thermal parameters for the C, N and O atoms, and isotropic thermal parameters for H(31) in (I), were refined using the *SHELXTL* system (Sheldrick, 1985).

Results and discussion

Conformation of diastereomers (I) *as acid and* (II) *as ethyl ester*

The chemical structure of the diastereomers (I) and (II) differ only in the configuration of C(18) (Fig. 1). Since all the other chiral centers in the diastereomers are the same as the natural product, the absolute configuration of the diastereomers could be assigned by placing the fused ring system into its known configuration (Lin, Li, Klayman, George & Flippen-Anderson, 1990; Qinghaosu Research Group, 1980). Thus, C(18) of (I) is in the R configuration, and C(18) of (II) is in the S configuration. The X-ray structure of the acid form of (I) was determined rather than the ethyl ester (I) due to the lack of a suitable crystal of (I). Table 1 gives the experimental details and Table 2 lists the coordinates and U_{eq} values for the non-H atoms and the acid H(31) atom for the acid form of diastereomer (I). Table 3 lists the coordinates and U_{eq} values for the non-H atoms of the two conformations of diastereomer (II), labeled molecule A and molecule B.*

The conformation of the fused ring system in both diastereomers is almost identical (Figs. 2*a–c*) and is virtually the same as that for dihydroartemisinin (β form) and β-artemether, where the ether group on C(10) is replaced either by a hydroxyl group or a methyl ether (Luo, Yeh, Brossi, Flippen-Anderson & Gilardi, 1984). Thus, in both diastereomers, the six-membered ring to which the ether sidechain is attached retains the chair conformation. This places the ether sidechain in an axial position and the methyl group attached to C(9) in an equatorial position. Both the alcohol function in dihydroartemisinin (β form) and the methyl ether in β-artemether are also in axial positions (Luo, Yeh, Brossi, Flippen-Anderson & Gilardi, 1984).

The endoperoxide is essential for antimalarial activity (Klayman, 1985). The peroxide O(1)—O(2) bond length ranges from 1.447(4) Å in the acid form of (I) to 1.477(7) and 1.474(13) Å for molecules A and B, respectively, in (II). The C(12a)—O(1)—O(2)—C(3) torsion angle ranges from 43.6 to 45.8° for the two diastereomers. The corresponding peroxide bond length and torsion angle in dihydroartemisinin (β form) and the ether analog β-artemether, both potent antimalarial agents, range from 1.442 to 1.479 Å and 44.2 to 46.2° (Luo, Yeh, Brossi, Flippen-Anderson & Gilardi, 1984).

The two crystalline conformations of (II) differ in the conformation of the flexible ether sidechain. Although the orientation of the ether sidechain is similar with the torsion angle C(10)—O(17)—C(18)—C(19) being −93.3(9)° and −107.2(9)° for molecules A and B, respectively, the phenyl ring of molecule A is twisted approximately 23° from the position of the phenyl ring in molecule B. Also, the ester in molecule A is rotated approximately 166° from the position of the ester in molecule B (see Figs. 2*b* and *c*), as shown by the torsion angle C(18)—C(28)—C(29)—O(30) of 128.2(1.3)° and −37.7(1.6)° for molecules A and B, respectively.

The difference in the conformation of the two diastereomers (I) and (II) is in the orientation of the nitrophenyl and acid/ester portions of the ether sidechain. In the acid form of (I), the phenyl ring points

* Lists of structure factors, anisotropic displacement parameters, H-atom coordinates and complete geometry have been deposited with the IUCr (Reference: CR0493). Copies may be obtained through The Managing Editor, International Union of Crystallography, 5 Abbey Square, Chester CH1 2HU, England.

Table 1. *Experimental details*

	(I)	(II)
Crystal data		
Chemical formula	$C_{24}H_{31}NO_9$	$C_{26}H_{35}NO_9$
Chemical formula weight	477.5	505.6
Cell setting	Monoclinic	Monoclinic
Space group	$C2$	$P2_1$
a (Å)	26.555 (3)	12.392 (2)
b (Å)	8.737 (1)	10.639 (2)
c (Å)	11.494 (1)	20.081 (2)
β (°)	114.32 (2)	91.51 (2)
V (Å^3)	2430.0 (5)	2646.5 (7)
Z	4	4
D_x (Mg m^{-3})	1.305	1.269
Radiation type	Cu $K\alpha$	Cu $K\alpha$
Wavelength (Å)	1.54184	1.54184
No. of reflections for cell parameters	25	25
θ range (°)	25–40	25–44
μ (mm^{-1})	0.84	0.80
Temperature (K)	298	298
Crystal form	Needles	Needles
Crystal size (mm)	0.35 × 0.12 × 0.06	0.40 × 0.17 × 0.10
Crystal color	Colorless	Colorless
Data collection		
Diffractometer	Siemens P4 four-circle	Siemens P4 four-circle
Data collection method	θ–2θ	θ–2θ
Absorption correction	None	None
No. of measured reflections	3761	4015
No. of independent reflections	1784	3805
No. of observed reflections	1680	2702
Criterion for observed reflections	$[\lvert F_o\rvert > 3\sigma(F)]$	$[\lvert F_o\rvert > 3\sigma(F)]$
R_{int}	0.009	0.023
θ_{max} (°)	114	114
Range of h, k, l	$-28 \rightarrow h \rightarrow 26$	$0 \rightarrow h \rightarrow 13$
	$-9 \rightarrow k \rightarrow 0$	$0 \rightarrow k \rightarrow 11$
	$0 \rightarrow l \rightarrow 12$	$-21 \rightarrow l \rightarrow 21$
No. of standard reflections	3	3
Frequency of standard reflections	Every 97 reflections	Every 97 reflections
Intensity decay (%)	5.5	3.8
Refinement		
Refinement on	F	F
R	0.050	0.064
wR	0.058	0.057
S	2.54	1.95
No. of reflections used in refinement	1680	2702
No. of parameters used	310	648
H-atom treatment	See text	See text
Weighting scheme	$w = [\sigma^2(\lvert F\rvert) + 0.00025(F_o)^2]^{-1}$	$w = [\sigma^2(\lvert F\rvert) + 0.00025(F_o)^2]^{-1}$
$(\Delta/\sigma)_{max}$	0.045	0.072
$\Delta\rho_{max}$ (e Å^{-3})	0.21	0.21
$\Delta\rho_{min}$ (e Å^{-3})	−0.25	−0.30
Extinction method	None	None
Source of atomic scattering factors	*SHELXTL-Plus*88 (Sheldrick, 1990)	*SHELXTL-Plus*88 (Sheldrick, 1990)
Computer programs		
Data collection	*P3/PC* (Siemens, 1989*a*)	*P3/PC* (Siemens, 1989*a*)
Cell refinement	*P3/PC* (Siemens, 1989*a*)	*P3/PC* (Siemens, 1989*a*)
Data reduction	*XDISK* (Siemens, 1989*b*)	*XDISK* (Siemens, 1989*b*)
Structure solution	*SHELXTL-Plus*88 (Sheldrick, 1990)	*SHELXTL-Plus*88 (Sheldrick, 1990)
Structure refinement	*SHELXTL-Plus*88 (Sheldrick, 1990)	*SHELXTL-Plus*88 (Sheldrick, 1990)
Preparation of material for publication	*SLIDEWRITE-Plus* (Advanced Graphics Software, Inc., Sunnyvale, California), Siemens Graphics Software (Madison, Wisconsin) and *SYBYL* (Tripos Associates, Inc., St Louis, Missouri)	*SLIDEWRITE-Plus* (Advanced Graphics Software, Inc., Sunnyvale, California), Siemens Graphics Software (Madison, Wisconsin) and *SYBYL* (Tripos Associates, Inc., St Louis, Missouri)

toward C(9) and lies under H(10) with the torsion angle C(10)—O(17)—C(18)—C(19) equal to 75.1 (0.4)°. Whereas in (II) the phenyl ring points toward O(11) and lies under H(12) with the torsion angle C(10)—O(17)—C(18)—C(19) equal to approximately −100°, as detailed in the above paragraph.

NMR analysis

The orientation of the phenyl rings in the crystal structures of (I) (acid form) and (II) explains the large differences in the chemical shifts of the H(10) and H(12) protons in the ^{1}H NMR spectra for (I) and (II) (see Fig.

Table 2. *Fractional atomic coordinates and equivalent isotropic displacement parameters* ($Å^2$) *for* (I)

$U_{eq} = (1/3)\sum_i\sum_j U_{ij} a_i^* a_j^* \mathbf{a}_i.\mathbf{a}_j.$

	x	y	z	U_{eq}
O(1)	0.5840 (1)	0.7511	0.6544 (3)	0.056 (1)
O(2)	0.6250 (2)	0.6494 (6)	0.7428 (3)	0.075 (2)
C(3)	0.6719 (2)	0.7347 (9)	0.8126 (5)	0.076 (2)
C(4)	0.6589 (2)	0.8803 (9)	0.8696 (5)	0.082 (3)
C(5)	0.6521 (2)	1.0205 (8)	0.7879 (5)	0.081 (3)
C(5a)	0.6083 (2)	1.0113 (7)	0.6494 (5)	0.061 (2)
C(6)	0.6128 (3)	1.1442 (8)	0.5673 (7)	0.100 (4)
C(7)	0.5727 (3)	1.1301 (9)	0.4312 (7)	0.109 (4)
C(8)	0.5765 (2)	0.9783 (8)	0.3727 (5)	0.082 (3)
C(8a)	0.5662 (2)	0.8458 (7)	0.4485 (4)	0.058 (2)
C(9)	0.5654 (2)	0.6852 (8)	0.3971 (4)	0.064 (2)
C(10)	0.6225 (2)	0.6310 (7)	0.4166 (3)	0.052 (2)
O(11)	0.6613 (1)	0.6513 (5)	0.5456 (2)	0.056 (1)
C(12)	0.6632 (2)	0.7963 (7)	0.6032 (4)	0.051 (2)
C(12a)	0.6068 (2)	0.8530 (6)	0.5893 (4)	0.044 (2)
O(13)	0.6998 (1)	0.7740 (6)	0.7312 (2)	0.078 (2)
C(14)	0.7098 (3)	0.6248 (12)	0.91296 (5)	0.136 (4)
C(15)	0.6069 (5)	1.2967 (9)	0.6247 (9)	0.151 (7)
C(16)	0.5244 (2)	0.6641 (12)	0.2577 (5)	0.115 (3)
O(17)	0.6403 (1)	0.7070 (5)	0.3315 (2)	0.046 (1)
C(18)	0.6796 (2)	0.6215 (7)	0.3026 (3)	0.048 (2)
C(19)	0.6509 (2)	0.4922 (7)	0.21110 (4)	0.049 (2)
C(20)	0.6062 (2)	0.5231 (8)	0.0967 (4)	0.072 (2)
C(21)	0.5788 (2)	0.4029 (9)	0.0171 (5)	0.084 (3)
C(22)	0.5955 (2)	0.2556 (9)	0.0540 (5)	0.071 (2)
C(23)	0.6395 (2)	0.2248 (8)	0.1625 (5)	0.086 (3)
C(24)	0.6671 (2)	0.3434 (8)	0.2416 (5)	0.068 (2)
N(25)	0.5633 (3)	0.1279 (11)	−0.0293 (7)	0.118 (4)
O(26)	0.5258 (3)	0.1604 (11)	−0.1307 (6)	0.198 (4)
O(27)	0.5776 (3)	−0.0015 (9)	0.0081 (7)	0.147 (4)
C(28)	0.7061 (2)	0.7356 (7)	0.2469 (4)	0.058 (2)
C(29)	0.7427 (2)	0.8476 (8)	0.3451 (4)	0.064 (2)
O(30)	0.7624 (2)	0.8274 (7)	0.4564 (3)	0.113 (2)
O(31)	0.7527 (2)	0.9697 (7)	0.2920 (3)	0.107 (2)
H(31)	0.7836 (28)	1.0595 (88)	0.3744 (60)	0.123 (22)

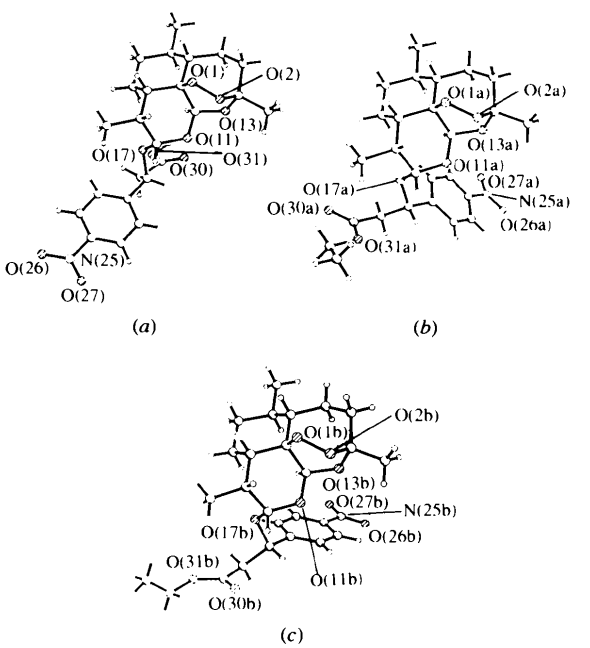

Fig. 2. Crystalline conformation of (*a*) the acid form of (I), (*b*) molecule *A* of (II) and (*c*) molecule *B* of (II). In all three drawings, the fused ring system is placed into the same orientation.

Table 3. *Fractional atomic coordinates and equivalent isotropic displacement parameters* ($Å^2$) *for* (II)

$U_{eq} = (1/3)\sum_i\sum_j U_{ij} a_i^* a_j^* \mathbf{a}_i.\mathbf{a}_j.$

	x	y	z	U_{eq}
O(1*A*)	0.5684 (4)	0.1166	0.9728 (2)	0.065 (2)
O(2*A*)	0.5758 (4)	0.2491 (7)	0.9515 (3)	0.068 (2)
C(3*A*)	0.5289 (7)	0.2592 (12)	0.8875 (5)	0.073 (4)
C(4*A*)	0.4188 (8)	0.1974 (12)	0.8807 (5)	0.084 (4)
C(5*A*)	0.4179 (7)	0.0638 (12)	0.8549 (4)	0.083 (4)
C(5a*A*)	0.4900 (7)	−0.0279 (10)	0.8944 (4)	0.065 (4)
C(6*A*)	0.5040 (8)	−0.1507 (12)	0.8553 (4)	0.079 (4)
C(7*A*)	0.5754 (8)	−0.2407 (11)	0.8924 (4)	0.082 (4)
C(8*A*)	0.6838 (8)	−0.1838 (11)	0.9113 (4)	0.077 (4)
C(8a*A*)	0.6727 (8)	−0.0677 (11)	0.9536 (4)	0.070 (4)
C(9*A*)	0.7761 (7)	−0.0034 (11)	0.9779 (4)	0.071 (4)
C(10*A*)	0.8311 (8)	0.0658 (11)	0.9221 (4)	0.075 (4)
O(11*A*)	0.7597 (5)	0.1481 (8)	0.8877 (3)	0.066 (2)
C(12*A*)	0.6581 (7)	0.1021 (11)	0.8652 (4)	0.065 (4)
C(12a*A*)	0.5962 (7)	0.0302 (10)	0.9199 (3)	0.055 (3)
O(13*A*)	0.5995 (4)	0.2060 (8)	0.8397 (2)	0.069 (2)
C(14*A*)	0.5261 (8)	0.4001 (11)	0.8741 (5)	0.097 (5)
C(15*A*)	0.3955 (8)	−0.2122 (12)	0.8377 (5)	0.110 (5)
C(16*A*)	0.8542 (9)	−0.0888 (13)	1.0170 (5)	0.106 (5)
O(17*A*)	0.8767 (4)	−0.0257 (8)	0.8786 (2)	0.068 (2)
C(18*A*)	0.9610 (6)	0.0197 (11)	0.8368 (4)	0.069 (3)
C(19*A*)	0.9179 (6)	0.0614 (11)	0.7698 (4)	0.061 (3)
C(20*A*)	0.8380 (7)	−0.0106 (10)	0.7359 (4)	0.063 (3)
C(21*A*)	0.8073 (6)	0.0174 (11)	0.6720 (4)	0.063 (3)
C(22*A*)	0.8545 (8)	0.1201 (12)	0.6418 (4)	0.067 (4)
C(23*A*)	0.9283 (7)	0.1936 (11)	0.6740 (5)	0.076 (4)
C(24*A*)	0.9594 (7)	0.1651 (12)	0.7374 (5)	0.072 (4)
N(25*A*)	0.8212 (7)	0.1484 (12)	0.5718 (4)	0.083 (4)
O(26*A*)	0.8563 (7)	0.2414 (10)	0.5468 (3)	0.117 (3)
O(27*A*)	0.7654 (7)	0.0749 (12)	0.5423 (3)	0.134 (4)
C(28*A*)	1.0351 (7)	−0.0930 (12)	0.8276 (4)	0.088 (4)
C(29*A*)	1.0844 (11)	−0.1431 (18)	0.8926 (7)	0.112 (7)
O(30*A*)	1.0784 (7)	−0.2545 (12)	0.9070 (4)	0.140 (4)
O(31*A*)	1.1265 (6)	−0.0604 (11)	0.9282 (4)	0.105 (4)
C(32*A*)	1.1751 (12)	−0.1018 (16)	0.9920 (7)	0.141 (8)
C(33*A*)	1.1919 (15)	−0.0134 (18)	1.0336 (7)	0.231 (12)
O(1*B*)	0.4494 (4)	0.1900 (9)	0.2864 (3)	0.078 (2)
O(2*B*)	0.4539 (5)	0.3181 (9)	0.3143 (3)	0.088 (3)
C(3*B*)	0.4954 (8)	0.3109 (13)	0.3797 (6)	0.085 (5)
C(4*B*)	0.5982 (7)	0.2309 (13)	0.3864 (5)	0.096 (5)
C(5*B*)	0.5772 (8)	0.0939 (13)	0.4052 (5)	0.092 (5)
C(5a*B*)	0.4986 (7)	0.0199 (12)	0.3585 (4)	0.072 (4)
C(6*B*)	0.4668 (8)	−0.1024 (12)	0.3907 (5)	0.082 (4)
C(7*B*)	0.3937 (7)	−0.1764 (11)	0.3414 (5)	0.084 (4)
C(8*B*)	0.2936 (7)	−0.1009 (11)	0.3217 (5)	0.081 (4)
C(8a*B*)	0.3247 (7)	0.0241 (11)	0.2904 (4)	0.068 (4)
C(9*B*)	0.2280 (7)	0.1057 (12)	0.2685 (4)	0.076 (4)
C(10*B*)	0.1802 (7)	0.1724 (11)	0.3266 (4)	0.071 (4)
O(11*B*)	0.2560 (5)	0.2406 (9)	0.3644 (3)	0.069 (2)
C(12*B*)	0.3474 (7)	0.1709 (11)	0.3889 (4)	0.073 (4)
C(12a*B*)	0.4040 (6)	0.1013 (11)	0.3328 (4)	0.061 (3)
O(13*B*)	0.4133 (4)	0.2593 (8)	0.4221 (3)	0.074 (2)
C(14*B*)	0.5109 (9)	0.4436 (13)	0.4011 (6)	0.118 (6)
C(15*B*)	0.5652 (8)	−0.1816 (14)	0.4113 (5)	0.119 (5)
C(16*B*)	0.1432 (8)	0.0381 (14)	0.2263 (4)	0.112 (5)
O(17*B*)	0.1214 (4)	0.0862 (8)	0.3661 (2)	0.062 (2)
C(18*B*)	0.0528 (6)	0.1473 (11)	0.4137 (4)	0.071 (4)
C(19*B*)	0.0998 (6)	0.1328 (12)	0.4838 (4)	0.060 (4)
C(20*B*)	0.1325 (6)	0.2362 (11)	0.5201 (5)	0.070 (4)
C(21*B*)	0.1702 (7)	0.2264 (13)	0.5845 (5)	0.079 (4)
C(22*B*)	0.1786 (6)	0.1083 (13)	0.6122 (4)	0.065 (4)
C(23*B*)	0.1496 (7)	0.0024 (12)	0.5777 (5)	0.080 (4)
C(24*B*)	0.1093 (7)	0.0159 (12)	0.5140 (5)	0.083 (4)
N(25*B*)	0.2195 (7)	0.0953 (15)	0.6816 (4)	0.090 (5)
O(26*B*)	0.2363 (7)	0.1904 (12)	0.7138 (4)	0.131 (4)
O(27*B*)	0.2332 (7)	−0.0095 (13)	0.7027 (4)	0.128 (4)
C(28*B*)	−0.0565 (6)	0.0853 (12)	0.4048 (4)	0.074 (4)
C(29*B*)	−0.1053 (9)	0.1188 (18)	0.3369 (5)	0.094 (5)
O(30*B*)	−0.0968 (7)	0.2205 (12)	0.3110 (4)	0.129 (4)
O(31*B*)	−0.1571 (6)	0.0244 (11)	0.3093 (3)	0.113 (4)
C(32*B*)	−0.2104 (14)	0.0465 (19)	0.2446 (7)	0.223 (11)
C(33*B*)	−0.1999 (15)	−0.0213 (17)	0.2003 (6)	0.228 (12)

3). The shielding/deshielding effect of the phenyl rings also explains the chemical shifts of the H(10) and H(12) atoms relative to the chemical shifts of the same H atoms in β-arteether, which contains no phenyl ring. In β-arteether, the ether group in the diastereomers is replaced by an ethyl ether function. For diastereomer (I) (Fig. 3*a*), the H(10) atom is positioned over the phenyl ring with a chemical shift of 4.56 p.p.m. The shielding effect of the phenyl ring results in a upfield shift of 0.24 p.p.m. from the 4.80 p.p.m. chemical shift of H(10) in β-arteether. For diastereomer (II) (Fig. 3*b*), the H(10) atom is positioned to the side of the phenyl ring with a chemical shift of 5.10 p.p.m. The deshielding effect of the phenyl ring results in a downfield shift of 0.30 p.p.m. from the chemical shift of H(10) in β-arteether.

The opposite case occurs for the H(12) atom. For diastereomer (I) (Fig 3*a*), the H(12) atom is positioned to the side of the phenyl ring with a chemical shift of 5.59 p.p.m. The deshielding effect of the phenyl ring results in a downfield shift of 0.18 p.p.m. from the 5.41 p.p.m. chemical shift of H(12) in β-arteether. For diastereomer (II) (Fig. 3*b*), the H(12) atom is positioned over the phenyl ring with a chemical shift of 4.79 p.p.m. The shielding effect of the phenyl ring results in an upfield shift of 0.62 p.p.m. from the chemical shift of H(12) in β-arteether. The shielding/deshielding effects of the phenyl ring on H(12) can only occur with the C(10) ether substituent in an axial position, since the phenyl ring cannot come in proximity to H(12) if the ether substituent occupies an equatorial position.

Packing

Since the NMR solution spectra are consistent with the crystalline conformation of the diastereomers, the conformation of (I) and (II) in solution appears to be similar to the crystalline conformation. Thus, the conformations observed in these crystal structures appear to be energetically favored since NMR indicates that these

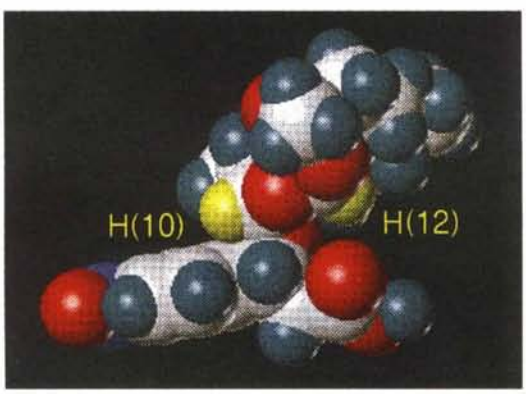

(*a*)

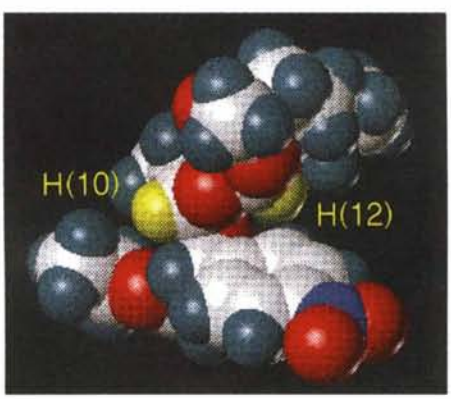

(*b*)

Fig. 3. Space-filling drawings representing 100% of the van der Waals radii showing the positioning of the nitrophenyl group relative to the H(10) and H(12) atoms in (*a*) the acid form of (I) and (*b*) molecule *A* of (II). The H(10) and H(12) atoms in each drawing have been colored yellow.

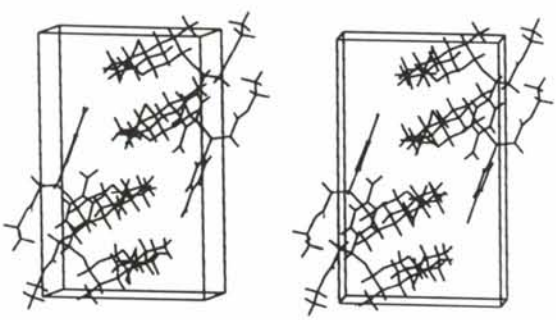

(*a*)

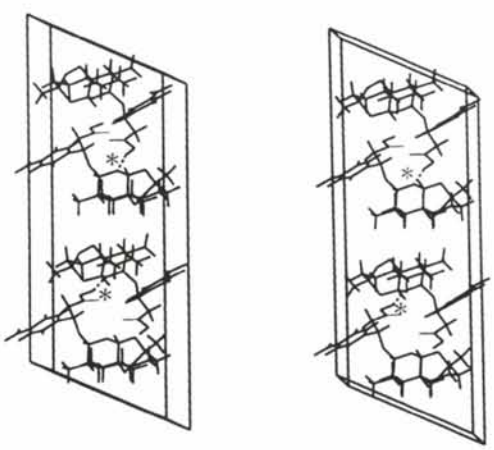

(*b*)

Fig. 4. (*a*) Stereo packing diagram of (II) where the *a* axis is horizontal and the *b* axis is vertical. (*b*) Stereo packing diagram of the acid form of (I) where the *c* axis is horizontal and the *a* axis is vertical. The asterisks are placed beside the dashed lines, indicating the hydrogen bonds between H(31) and O(11) of neighboring molecules.

conformations persist in solution. Diastereomer (II) has no hydrogen bonds and packs with no intermolecular distances less than van der Waals distances (Fig. 4*a*).

Unlike (II), the acid form of (I) has an acid H atom available for hydrogen bonding. This H atom makes a hydrogen bond to the ether O(11) atom, as illustrated in Fig. 4(*b*). The O(31)···O(11) distance is 2.776(9), O(31)—H(31) = 1.24(6), H(31)···O(11) = 1.59(6) Å, and the O(31)—H(31)···O(11) angle is 156.7(3.5)° (symmetry code: $\frac{3}{2}-x, \frac{1}{2}+y, 1-z$). Although an ether O atom is a less commonly observed hydrogen-bond acceptor than a hydroxyl or ketone group, the O(31)···O(11) distance and O(31)—H(31)···O(11) angle is equal to the mean $O_d\cdots O_a$ distance of 2.7667 ± 0.0700 Å and close to the mean $O_d—H\cdots O_a$ angle of 167.11 ± 6.53° observed from neutron diffraction data for 74 linear hydrogen bonds, nine involving a $C—O_a—C$ acceptor (Ceccarelli, Jeffrey & Taylor, 1981).

References

CECCARELLI, C., JEFFREY, G. A. & TAYLOR, R. (1981). *J. Mol. Struct.* **70**, 255–271.

KARLE, J. & KARLE, I. L. (1966). *Acta Cryst.* **21**, 849–859.

KLAYMAN, D. L. (1985). *Science*, **228**, 1049–1055.

LIN, A. J., LI, L., KLAYMAN, D. L., GEORGE, C. F. & FLIPPEN-ANDERSON, J. L. (1990). *J. Med. Chem.* **33**, 2610–2614.

LUO, X., YEH, H. J. C., BROSSI, A., FLIPPEN-ANDERSON, J. L. & GILARDI, R. (1984). *Helv. Chim. Acta*, **67**, 1515–1522.

Qinghaosu Research Group (1980). *Sci. Sin. (Engl. Ed.)* **23**, 380–396.

SHELDRICK, G. M. (1985). *SHELXS86. Crystallographic Computing* 3, edited by G. M. SHELDRICK, C. KRÜGER & R. GODDARD, pp. 175–189. Oxford Univ. Press.

SHELDRICK, G. M. (1990). *SHELXTL-Plus88 Structure Determination Software Programs*. Nicolet Instrument Corporation, Madison, Wisconsin, USA.

Siemens (1989*a*). *P3/PC Diffractometer Program*. Version 3.13. Siemens Analytical X-ray Instruments Inc., Madison, Wisconsin, USA.

Siemens (1989*b*). *XDISK. Data Reduction Program*. Version 3.11. Siemens Analytical X-ray Instruments Inc., Madison, Wisconsin, USA.

Acta Cryst. (1995). B**51**, 1068–1081

Correlation of the Hydrogen-Bond Acceptor Properties of Nitrogen with the Geometry of the Nsp^2→Nsp^3 Transition in $R_1(X{=})C—NR_2R_3$ Substructures: Reaction Pathway for the Protonation of Nitrogen

BY FRANK H. ALLEN,* CRAIG M. BIRD AND R. SCOTT ROWLAND

Cambridge Crystallographic Data Centre, 12 Union Road, Cambridge CB2 1EZ, England

AND STEPHANIE E. HARRIS AND CARL H. SCHWALBE

Pharmaceutical Sciences Institute, Aston University, Aston Triangle, Birmingham B4 7ET, England

(*Received* 24 *February* 1995; *accepted* 4 *April* 1995)

Abstract

The non-bonded N···H interactions between N atoms of $R_1(X{=})C—N(R_2R_3)$ (R_2,R_3 = Csp^3 or H) substructures and the H atoms of N—H and O—H donors have been analysed using crystallographic data and *ab initio* molecular orbital calculations. A total of 946 contacts having N···H (d_{NH}) ≤ 2.75 Å were retrieved from the Cambridge Structural Database. For the preferred all-planar (Nsp^2) conformation, d_{NH} ranges upwards from *ca* 2.5 Å and H approaches N approximately perpendicular to the plane. However, it is shown that close intramolecular steric interactions lead to major geometrical distortions [pyramidalization at N and rotation about the C—N bond: Ferretti, Bertolasi, Gilli & Gilli (1993). *J. Phys. Chem.* **49**, 13568–13574]. The N atom undergoes a transition from sp^2 to sp^3 with gradual lone-pair formation on N. If N-pyramidality is measured by χ_N (the angle between the C—N vector and the NR_2R_3 plane), then as χ_N increases beyond *ca* 35° towards the sp^3 value of *ca* 60° the N···H contacts tend to become significantly shorter (stronger), the N···H donor angle approaches linearity and H approaches N within a 20° cone that has the assumed N lone-pair vector as an axis. A plot of χ_N *versus* d_{NH} is interpreted as the reaction pathway for protonation of N and data points from $R_1(X{=})C—N^+(R_2R_3)H$ systems (the reaction product) occur at the end of this pathway. Crystallographic evidence shows that all 153 contacts ≤ 2.75 Å that have $\chi_N \geq 35°$ and a N···H donor angle above 130° are true hydrogen bonds. The evidence also suggests that the incoming H atoms track the developing N lone-pair density as χ_N increases from *ca* 35 to 60°. *Ab initio* molecular orbital calculations for aniline (6–31 G* basis

* Author to whom correspondence should be addressed.